A Journal of the Gesellschaft Deutscher Chemiker

Angewandte International Edition GDCh Chemie

www.angewandte.org

Accepted Article

Title: Superprotonic Conduction over Wide Humidity Range Driven by Enhanced Proton Dissociation

Authors: Kun Zhang, Lei Wu, Ke Gong, Shuyang Bian, Yanting Zhang, Huayu Gu, Dongshuang Wu, Linfeng Hu, Huiyuan Liu, and Yusong Wang

To be cited as: *Angew. Chem. Int. Ed.* **2025**, e202421444

Link to VoR: https://doi.org/10.1002/anie.202421444

WILEY VCH

Superprotonic Conduction over Wide Humidity Range Driven by Enhanced Proton Dissociation

Kun Zhang[+*], Lei Wu[+], Ke Gong[+], Shuyang Bian[+], Yanting Zhang, Huayu Gu, Dongshuang Wu, Linfeng Hu[*], Huiyuan Liu[*], Yusong Wang[*]

[*]L. Wu, Y. Zhang, Prof. K. Zhang

Automotive Engineering Research Institute, Jiangsu University

301 Xuefu Road, Zhenjiang, 212013 (P. R. China)

E-mail: kunzhang@ujs.edu.cn

Dr. K. Gong, Prof. Y. Wang

Hefei National Research Center for Physical Sciences at the Microscale, University of Science and Technology of China

373, Mount Huangshan Road, Hefei, 230026 (P. R. China)

E-mail: wangys@ustc.edu.cn

Prof. H. Liu

Institute for Energy Research, Jiangsu University

301 Xuefu Road, Zhenjiang, 212013 (P. R. China)

E-mail: huiyuanliu@ujs.edu.cn

S. Bian, Prof. L. Hu

School of Materials Science and Engineering, Southeast University

Energy Storage Center, Southeast University

2 Southeast University Road, Nanjing City, 211189 (P. R. China)

E-mail: linfenghu@seu.edu.cn

H. Gu, D. Wu

School of Material Science and Engineering, Nanyang Technological University,

50 Nanyang Avenue, 639798 (Singapore)

[+]These authors contributed equally to this work.

ABSTRACT: Proton conducting materials play a key role in various fields, and their proton conduction is profoundly restricted by the proton dissociation process. This process has two components: dissociation from acidic groups (e.g. -SO_3H) and dissociation from intermediate species (e.g. H_3O^+, C-F···H^+). Extensive research has concentrated on the former, utilizing acidic groups with minimal proton dissociation energy or low pKa values, while the latter's substantial effects have been largely overlooked. In reality, proton-accepting atoms within intermediates, such as oxygen and nitrogen, typically produce a higher electron cloud density compared to those in acidic groups. This results in a pronounced electrostatic binding effect on mobile protons, as well as high dissociation energies. Thus, diminishing the dissociation energy associated with intermediates is paramount in the development of high-performance proton conductors. Herein, we construct one covalent organic framework based proton conductor, achieving superprotonic conduction over wide humidity range by decreasing the dissociation energy of protons from intermediates. The success of this approach can be attributed to two key factors: the crowded guest molecules within the framework that mitigate proton hydration, and the concurrent establishment of C-H···H^+ interactions. These combined effects significantly reduce the electrostatic attraction exerted on mobile protons, thereby enhancing proton conduction.

Introduction

Proton-conducting materials have garnered significant attention from researchers due to their crucial role in various fields, including sensing,[1] fuel cells,[2] biomaterial transport[3] and pseudocapacitors.[4] Their proton conductivity (σ) is determined by diffusion velocity and carrier concentration, as described by Einstein's equation:

$$\sigma = \frac{q^2 nD}{k_B T} \quad (1)$$

where q, D, n, k_B, and T represent the charges, diffusion constant, carrier concentration, Boltzmann constant and absolute temperature.[5] Based on this, mainstream research on proton conduction can be categorized into two approaches: firstly, enhancing the diffusion rate by constructing tight hydrogen bond networks or creating special confined environments to alter the dynamic properties of charge carriers;[6] and secondly, increasing the concentration of carriers by utilizing acidic groups with low proton dissociation energy and maximizing

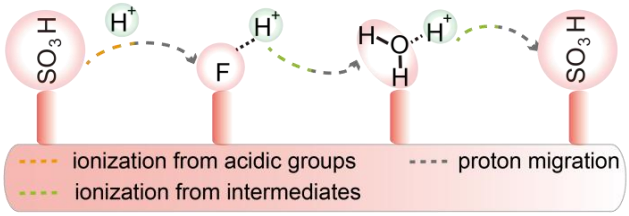

Figure 1. Different processes in proton conduction. F represents the fluorine atom on the C-F bond.

10.1002/anie.202421444

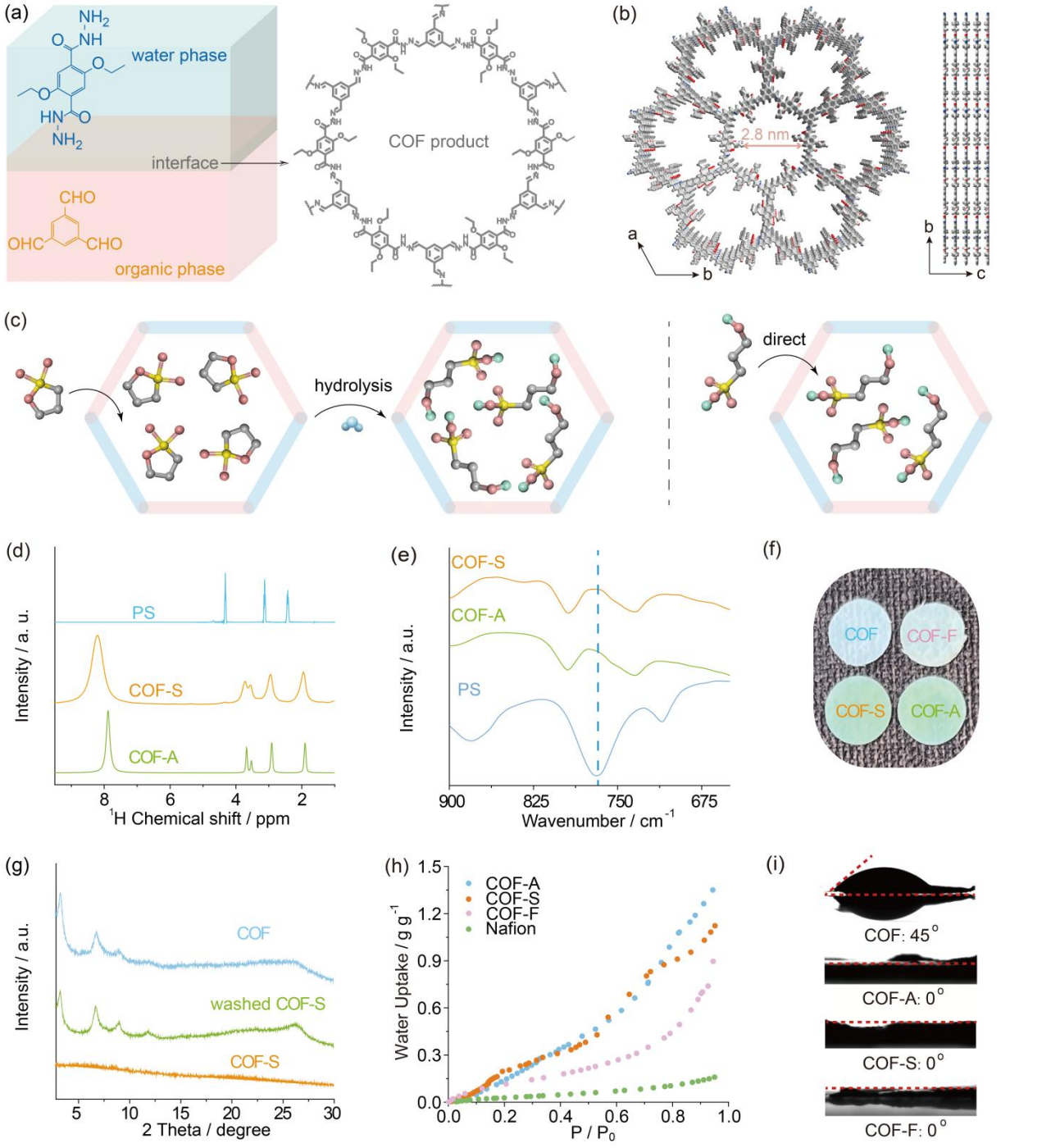

Figure 2. (a) Schematic diagram of interfacial polymerization process of COF membrane. (b) 2D structure of COF framework. (c) Schematic illustration of introducing hydroxypropanesulfonic acid by hydrolysis reaction and direct loading respectively. (d) Solid-state ^{1}H NMR of various samples. (e) IR plot with C-S stretching vibration. (f) Photos of COF, COF-F, COF-S and COF-A membranes. (g) PXRD spectra of COF, COF-S and washed COF-S. (h) Water adsorption of Nafion, COF-F, COF-S and COF-A. (i) Water contact angle of COF, COF-F, COF-A and COF-S.

their spatial density.[7] Overall, these studies focus on two processes in proton conduction: the dissociation of protons from acidic groups and their migration between relay sites. In fact, proton transfer also involves the dissociation of intermediates (e.g. H_3O^+, C-F$\cdots$H$^+$ and -NH_2^+-) (Figure 1).[8] And this process is important to the total dissociation energy, which will significantly influence charge carrier concentration and, consequently, proton conductivity. However, research in this area still remains scarce.

Theoretically, intermediates such as hydrated protons can facilitate proton diffusion by providing multiple transfer sites.[9] But they increase the dissociation energy at same time due to the high-density electron cloud on proton-accepting atoms strongly attracting mobile protons.[10] This also implies that the diffusion loss caused by reduction of intermediates (e.g. H_3O^+) can be partly compensated by simultaneously decreased dissociation energy. Such speculation may offer solutions to critical proton conduction

10.1002/anie.202421444

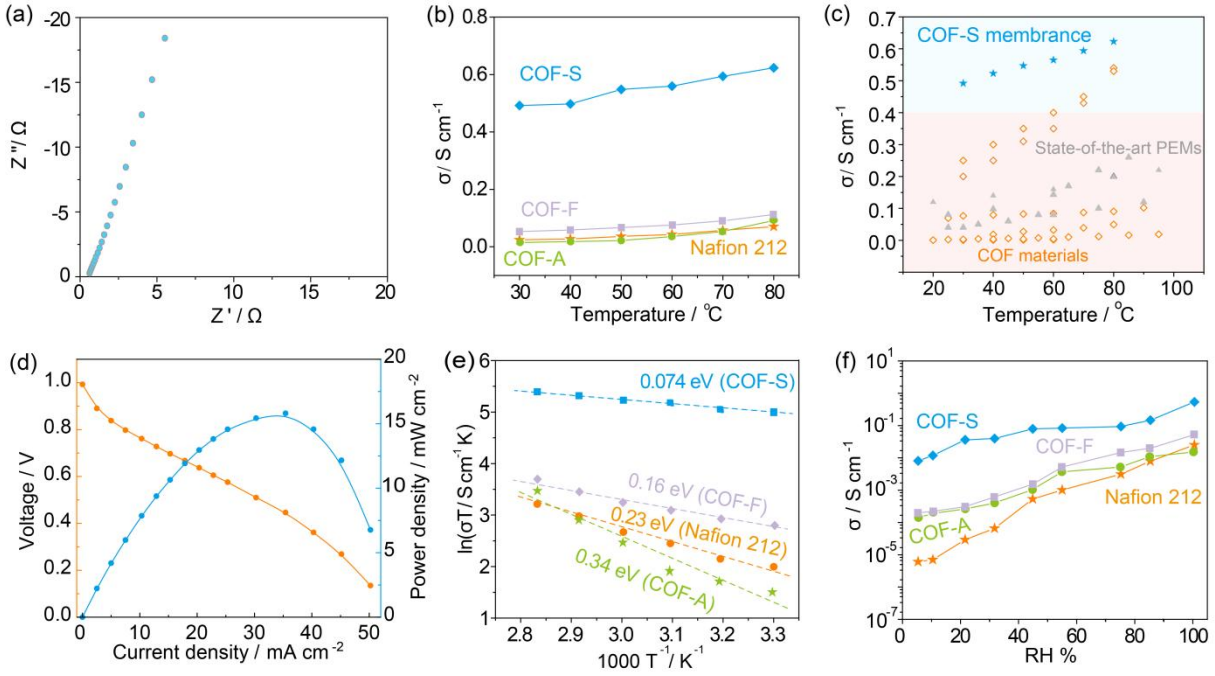

Figure 3. (a) Nyquist plot of COF-S under 100% RH and 80 °C. (b) Proton conductivity at 100% RH versus different temperatures. (c) Comparison of proton conductivity data for COF-S, COF materials[14] and state-of-the-art PEMs.[15] (d) Performance of the H_2/O_2 fuel cell at 60 °C and 100% RH. (e) Activation energy of various samples at 100% RH. (f) Proton conductivity of COF-F, COF-S, COF-A and Nafion at 30 °C versus various RH.

issues, including inefficient proton conduction of commercial proton exchange membranes (PEMs) stemming from diminished proton diffusion in low humidity.[11] On the flip side, it has been shown that the presence of positively charged areas within a structure enhances the transference number or conductivity of cations,[12] mainly due to the reduced electrostatic attraction and consequentially lowered dissociation energies.

Based on the analysis above, we saturated hydroxypropanesulfonic acid within nanospace, utilizing its methyl groups to construct positive-to-positive interactions (C-H···H^+), and controlling the hydration degree through crowding effect. The nanospace is provided by one 2D covalent organic framework (COF), chosen due to its high porosity and 1D channel facilitating proton transfer. The resulting composite exhibits a low proton dissociation energy, conferring it with a minimally humidity-dependent proton conductivity that outperforms commercial PEMs, reaching a peak value of 6.23×10^{-1} S cm^{-1} at 80 °C and 100% RH.

Results and Discussion

The COF membrane was prepared by interfacial polymerization (Figure 2a), which has the same structure as COF-42 based on simulation (Figure S1, Table S1),[13] but possesses a macroscopic membrane form that facilitates the assembly of subsequent device (fuel cell). Due to the AA stacking of P_3 (143) space group, the membrane has 2D structure with 1D channel (pore size of 2.8 nm) that can accommodate guest molecules for proton conduction (Figure 2b, Figure S2). The membrane was then immersed in 1,3-propane sultone (PS), and finally exposed to a humid environment to complete hydrolysis and obtain product COF-S (left in Figure 2c). As a comparison, hydroxypropanesulfonic acid (HA) is directly introduced into the membrane to obtain COF-A (right in Figure 2c), which possesses 5.21 HA per pore (based on S/N in Table S2). As seen in Figure 2d, the ^{1}H characteristic peaks of PS in COF-S is notably faint, whereas that of HA is quite pronounced in COF-S. The yield of hydrolysis (β) reaches 93.7% (Figure S3 and "NMR calculation" section in supporting information), corresponding to 6.56 HA and 0.44 PS per pore (based on Table S2 and β). This indicates that the vast majority of PS in COF-S has completed hydrolysis. Meanwhile, the C-S stretching vibration has significant displacement, from 768 cm^{-1} of bulk PS to 794 cm^{-1} of COF-S and COF-A, confirming the hydrolysis again (Figure 2e, Figure S4). The larger amount of HA within COF-S is probably because the precursor (PS) exhibits decreased steric bulk and weaker intermolecular hydrogen bonding compared to its hydrolyzed product (HA), which will promote the penetration of more guest molecules into the nanospace. No obvious structural alterations are observed between washed COF-S and COF based on IR and ^{13}C NMR (Figure S5 and Figure S6), and TG plot of COF-S gives weight-loss process of HA between approximate 100 °C and 200 °C (Figure S8). These demonstrate that HA molecules reside within the pores as guest molecules, rather than being grafted onto the frameworks as functional groups. The different contents of HA lead to varying degrees of pore congestion in COF-S and COF-A, which is advantageous for controlling the hydration of protons on -SO_3H under humid conditions, and illustrating the influence of hydration to proton conduction. On the other hand, to elucidate the effect of C-H···H^+ in COF-S on proton conduction, COF-F (COF incorporated with CF_3SO_3H) and Nafion with C-F bonds are added as comparison. The macroscopic and microscopic morphology of COF based samples are shown in Figure 2f and Figure S9. The diffraction peaks reappear after COF-F, COF-S and COF-A being washed (Figure 2g, Figure S10), indicating remained porous structure. Despite the decreased nitrogen adsorption (Figure S11), the

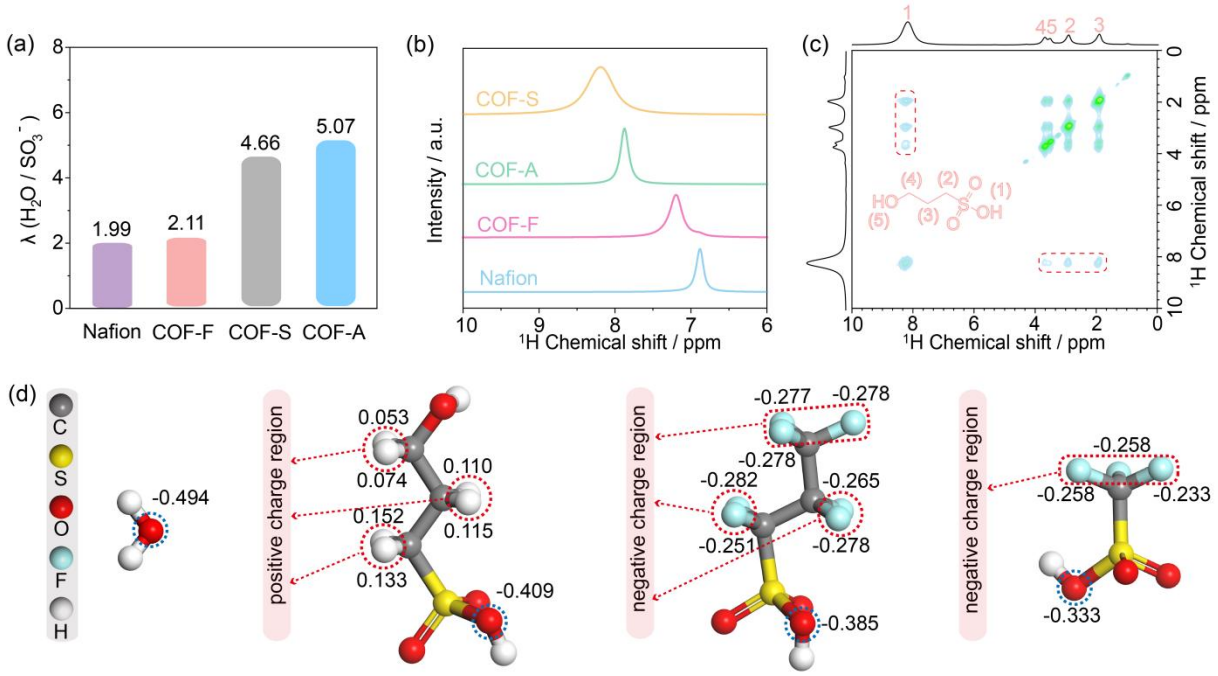

Figure 4. (a) Hydration degree of COF-F, Nafion, COF-A and COF-S at 32% RH. (b) Active proton of different samples in solid-state ^{1}H NMR at 32% RH. (c) 2D ^{1}H-^{1}H NOESY spectrum of COF-S, with active proton coupling behaviour within red dashed area. (d) Charge of H on C-H (red dashed), F on C-F (red dashed), and O on -SO_3H and water (blue dashed). Molecules from left to right are water, HA, a small molecule similar to Nafion fragment, and CF_3SO_3H.

water adsorption of COF-F, COF-S, and COF-A is increased (Figure 2h and Figure S12), which is caused by the HA molecules that make the membrane more hydrophilic (Figure 2i).

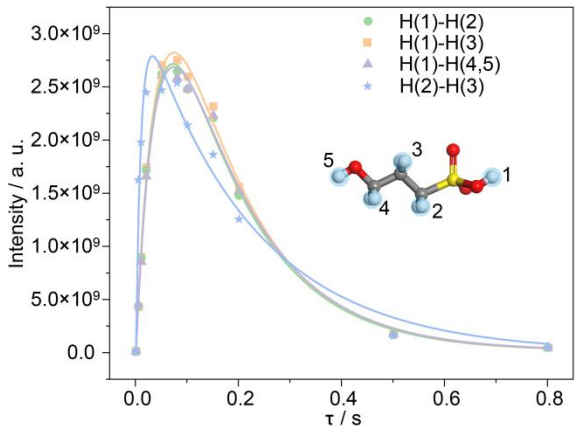

Figure 5. The ^{1}H-^{1}H HOESY with different mixing time of COF-S at 32% RH.

Proton transport behavior is assessed through electrochemical impedance spectroscopy (EIS) (Figure 3a, Figure S13-S28). The structures have no obvious changes after the measurement (Figure S29). The proton conductivity of COF-S reaches a maximum value of 6.23×10^{-1} S cm^{-1} at 80 °C and 100% RH, which is higher than that of Nafion 212 (7.04×10^{-2} S cm^{-1}), COF-F (1.21×10^{-1} S cm^{-1}) and COF-A (9.10×10^{-2} S cm^{-1}) (Figure 3b). This value is currently the highest among the proton-conducting materials ((Figure 3c, Table S3-S5). One H_2/O_2 fuel cell is assembled with COF-S as solid-state electrolyte via gas diffusion electrode (GDE) method and operates successfully (Figure S30, Figure 3d). The maximum open circuit voltage (OCV) is up to 1 V and maximum powder density achieves 16 mW cm^{-2}, confirming the proton conduction function of COF-S and demonstrating the possibility of practical application. The activation energy at 100%RH is only 0.074 eV for COF-S, which is much lower than that of Nafion (0.23 eV), COF-F (0.16 eV) and COF-A (0.34 eV) (Figure 3e), and represents one near pure Grotthuss-type proton conducting mechanism. Such low activation energy can as well avoid prolonged start-up time for automobile applications and translates to stable proton conductivity over a wide range of temperature.[16] The proton conductivity of Nafion 212 declines dramatically from 2.43×10^{-2} S cm^{-1} at 100% RH to 6.53×10^{-6} S cm^{-1} at 6% RH (Figure 3f). This exponential decay, commonly observed in conventional PEMs, with amagnitude of 2 to 3 orders, serves as a significant bottleneck in the practical application.[17] However, COF-S exhibits weakly humidity-dependent proton conduction. The proton conductivity only marginally decreases and maintains over ~10^{-3} S cm^{-1} from 100% RH to 6% RH, being several orders of magnitude higher than conventional PEMs.

The dissociation process of protons is crucial for proton conduction. Hence, we meticulously analyze the factors influencing proton dissociation, beginning with the hydrated proton. The hydration degree can be quantified by the number of water molecules per sulfonic group, denoted as λ. λ at 32% RH is 4.66 and 5.07 for COF-S and COF-A (Figure 4a, "λ calculation" section in SI). Meanwhile, the active proton signal of COF-S is located at a lower field compared to that of COF-A (8.19 ppm for COF-S, 7.88 ppm for COF-A at 32% RH) (Figure 4b). The signal of the active protons in COF-S shifts to lower fields at 7% RH (λ=0.79) compared to 32% RH (λ=4.66) (Figure S7). Such phenomenon of proton signal of -SO_3H shifting toward lower field with lower degree of hydration also occurs in Nafion.[18] This is because oxygen atoms in water carry a more negative charge than those in -SO_3H (blue dashed in Figure 4d), resulting in a higher electron cloud density around

hydrated protons than around protons in -SO_3H. Therefore, the lower hydration degree is beneficial for diminishing the electron density around mobile protons, which can further decrease Coulombic attraction to proton and proton dissociation energy. Despite the fact that low hydration reduces hydrogen bonding, which would lead to a shift of proton signals to a higher field, it is clear that in -SO_3H systems, the effect of hydration level is more pronounced than that of hydrogen bonding. It's worth noting that the λ values for Nafion and COF-F are 1.99 and 2.11, respectively (at 32% RH, Figure 4a), which are both lower than that of COF-S (λ=4.66). However, COF-S with larger λ still has active proton signal sitting at lower field compared to Nafion and COF-F (8.19 ppm for COF-S, 7.19 ppm for COF-F and 6.88 ppm for Nafion at 32% RH) (Figure 4b). This is attributed to the presence of C-H···H^+ interactions in COF-S, whereas Nafion and COF-F exhibit C-F···H^+ interactions. The C-H group carries a positive charge, which is opposite to that of the C-F group (red dashed in Figure 4d). Therefore, the C-H···H^+ interaction can reduce the electron density surrounding active protons, causing the signal to shift towards the low field. This can simultaneously weaken the Coulombic force acting on the proton and reduce the proton dissociation energy. The existence of C-H···H^+ interaction is further proved by 2D ^{1}H-^{1}H NOESY (32% RH) in Figure 4c, where the active proton exhibits a significant coupling behaviour with C-H.

The ^{1}H-^{1}H HOESY with different mixing time of COF-S is shown in Figure 5, illustrating the interaction between H(1) and H(3), and between H(2) and H(3). The curves were fitted using an exponential function derived from the fundamental Solomon equation,[19] using r (total longitudinal relaxation rate constant) and η as fit-able parameters:

$$\mathrm{NOE} = \frac{1}{2}\exp[-(r-\eta)\tau][1-\exp(-2\eta\tau)] \quad (2)$$

The obtained parameters are shown in Table S6. The 6th power of distance (d) between two interacting hydrogen atoms is inversely proportional to η.[20] Therefore, the relationship can be obtained:

$$\frac{d_{[\mathrm{H(1)-H(3)}]}^{6}}{d_{[\mathrm{H(2)-H(3)}]}^{6}} = \frac{\eta_{[\mathrm{H(2)-H(3)}]}}{\eta_{[\mathrm{H(1)-H(3)}]}} \quad (3)$$

$d_{[\mathrm{H(2)-H(3)}]}$ can be directly observed based on its molecular structure, which is 2.51 Å, thus the calculation result of $d_{[\mathrm{H(1)-H(3)}]}$ is 3.36 Å. By this method, $d_{[\mathrm{H(1)-H(2)}]}$ and $d_{[\mathrm{H(1)-H(4,5)}]}$ is 3.32 Å and 3.33 Å, respectively. It should be noted that this value is an average, encompassing all C-H···H^+ interactions ranging from 0 to 5 Å. The radial distribution function (RDF) shows that the C-H···H^+ starts from 1.5 Å, and obvious peaks appear at 2.5 Å, 3.6 Å and 4.6 Å, demonstrating that the C-H···H^+ exist from short distance to middle distance, and to long distance (Figure S31).

The $d_{[\mathrm{H(1)-H(3)}]}$, $d_{[\mathrm{H(1)-H(2)}]}$ and $d_{[\mathrm{H(1)-H(4,5)}]}$ are 3.41 Å, 4.03 Å and 4.30 Å for COF-A, respectively (Figure S32), illustrating slightly weaker C-H···H^+ interactions. The ^{1}H-^{19}F HOESY of COF-F and Nafion also demonstrates the C-F···H^+ interaction (Figure S33-S34). Due to the lack of reference standards such as H(2)-H(3) in ^{1}H-^{1}H HOESY, the distance of F and H ($d_{\mathrm{F-H}}$) can not be calculated. However, it can be confirmed that their interaction distance must be less than 5 Å, as this is the range where NOE signals appear. According to the equation of electrostatic force:

$$F = k\frac{Qq}{d^2} \quad (4)$$

here Q is the charge of H on C-H or F on C-F (Averaged charge is +0.106 for H, and -0.250 for F. Figure 4d), q is the charge of proton, d is the interaction distance obtained from HOESY (estimating $d_{\mathrm{F-H}}$ within the range of 1.5-5 Å), k is electrostatic constant, the electrostatic repulsion between C-H and H^+ is in the same order of magnitude as the electrostatic attraction between C-F and H^+. This indicates that the C-H···H^+ interaction can indeed prevent the proton from being bound by the negative charge, and reduces proton dissociation energy. Compared to the F system, the effective role of the H system is the sum of the attractive force (C-F···H^+) and the repulsive force (C-H···H^+), which can not be ignored. On the hand, the molecular dynamics calculation shows that the diffusion coefficient is 3.12×10^{-10} m^2 s^{-1} and 2.57×10^{-9} m^2 s^{-1} for COF-S and COF-F (Figure S35). Combining Einstein's equation (equation (1)), the mobile proton concentration is 1.98×10^{23} / m^3 and 3.89×10^{20} / m^3 for COF-S and COF-F. Considering that COF-S possesses lower -SO_3H concentration than COF-F (4.09 / nm^3 and 2.60 / nm^3 for COF-F and COF-S, calculated in "-SO_3H concentration" section in supporting information), the higher mobile proton concentration of COF-S is due to its lower proton dissociation energy.

Further, we excluded the influence of hydration and discussed the effect of C-H···H^+ and C-F···H^+ in detail. COF-F, COF-S and Nafion were then measured by one broadband dielectric spectrometer in anhydrous condition (Figure S36-S37 and Table S7-S8). COF-S exhibits the highest proton conductivity and carrier concentration (left and right of Figure 6a), yet it has the lowest diffusion constant (in the middle of Figure 6a). According to Arrhenius law (Figure S38), the activation energy of proton conductivity (E_a) is 0.52 eV, 0.19 eV and 0.27 eV, and the activation energy for proton migration (E_m) is 0.01 eV, 0.02 eV and 0.19 eV, for Nafion, COF-F and COF-S respectively (Figure 6b). The E_f (energy required to form mobile protons) is obtained based on $E_f = E_a - E_m$,[21] which is 0.51 eV, 0.17 eV and 0.08 eV for Nafion, COF-F and COF-S (Figure 6b).

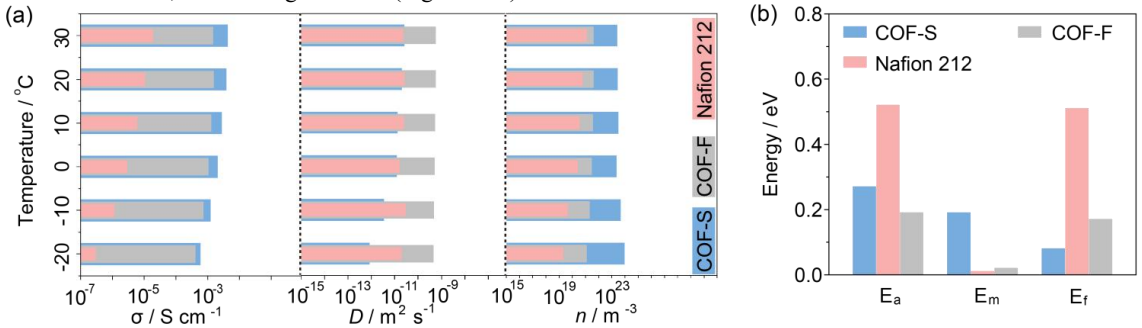

Figure 6. (a) Proton conductivity (left), diffusion constant (middle) and carrier concentration (right) for COF-S, COF-F and Nafion in nitrogen. (b) Mobile proton formation energy, proton migration energy and total energy.

Considering that the pKa value of -SO_3H in COF-S is higher due to the absence of the electron-withdrawing effect of fluorine atoms, which means that the energy required for proton ionization from -SO_3H in COF-S is larger, its smaller E_f value is attributed to the contribution of C-H$\cdots$$H^+$ interactions. On the other hand, the mobile proton concentration is determined by acidic group concentration and E_f. Although COF-S possesses lower -SO_3H concentration than COF-F (4.09 / nm^3 and 2.60 / nm^3 for COF-F and COF-S, calculated in "-SO_3H concentration" section in supporting information), it has higher mobile proton concentration than COF-F, demonstrating the significant role of C-H$\cdots$$H^+$ in decreasing E_f and improving proton concentration.

Conclusion

To sum up, COF-S obtains a weakly humidity-dependent proton conductivity, with a maximum value of 6.23×10^{-1} S cm^{-1} at 80 °C and 100% RH, which is superior to commercial proton exchange membrane Nafion. Its weakened hydration and C-H$\cdots$$H^+$ interactions significantly reduce the proton dissociation energy and contribute to proton conduction. Differing from the previous studies that focused on the pKa of acidic groups or proton diffusion for proton conductivity, our research demonstrates the importance of reducing proton dissociation energy of H_3O^+, -NH_3^+, C-F$\cdots$$H^+$, et al, and provides new insights for the synthesis of high-performance proton conducting materials.

Acknowledgment

This work was supported by National Natural Science Foundation of China (52207238, 52171203, 52371214), the Natural Science Foundation of Jiangsu Province (BK20211516), China Postdoctoral Science Foundation (2023M731361) and Jiangsu University Senior Talent Launch Fund.

Conflict of Interest

The authors declare no conflict of interest.

Data Availability Statement

The data that support the findings of this study are available from the corresponding author upon reasonable request.

Keywords: Covalent Organic Framework · Proton Conducting Intermediates · Dissociation Energy · Weakly Humidity-Dependent Superprotonic Conductivity

[1] K. Zhang, X. Xie, H. Li, J. Gao, L. Nie, Y. Pan, J. Xie, D. Tian, W. Liu, Q. Fan, H. Su, L. Huang, W. Huang, *Adv. Mater.* **2017**, *29*, 1701804.

[2] a) Z. Xie, L. Tian, W. Zhang, Q. Ma, L. Xing, Q. Xu, L. Khotseng, H. Su, *Int. J. Hydrogen. Energ.* **2021**, *46*, 10903-10912; b) S. Lin, S. A. Kedzior, J. Zhang, M. Yu, V. Saini, R. P.S. Huynh, G. K.H. Shimizu, M. Trifkovic, *Chem* **2023**, *9*, 2547-2560.

[3] S. Lin, J.-Y. Tsai, C.-D. Hsiao, Y. Huang, C.-L. Chiu, M. Liu, J.-Y. Tung, T. Liu, R. Pan, Y. Sun, *Nature* **2012**, *484*, 399-403.

[4] Y. Yang, P. Zhang, L. Hao, P. Cheng, Y. Chen, Z. Zhang, *Angew. Chem. Int. Ed.* **2021**, *60*, 21838-21845; *Angew. Chem.* **2021**, *133*, 22009 -22016.

[5] D.-W. Lim, H. Kitagawa, *Chem. Rev.* **2020**, *120*, 8416-8467.

[6] a) S. Bureekaew, S. Horike, M. Higuchi, M. Mizuno, T. Kawamura, D. Tanaka, N. Yanai, S. Kitagawa, Nat. Mater. **2009**, *8*, 831-836; b) K.-i. Otake, K. Otsubo, T. Komatsu, S. Dekura, J. M. Taylor, R. Ikeda, K. Sugimoto, A. Fujiwara, C.-P. Chou, A. W. Sakti, Y. Nishimura, H. Nakai, H. Kitagawa, *Nat. Commun.* **2020**, *11*, 843; c) G. Hummer, J. C. Rasaiah, J. P. Noworyta, *Nature* **2001**, *414*, 188-190; d) F. Zhang, L. Dong, J. Qin, W. Guan, J. Liu, S. Li, M. Lu, Y. Lan, Z. Su, H. Zhou, *J. Am. Chem. Soc.* **2017**, *139*, 6183-6189; e) Y. Ye, W. Guo, L. Wang, Z. Li, Z. Song, J. Chen, Z. Zhang, S. Xiang, B. Chen, *J. Am. Chem. Soc.* **2017**, *139*, 15604-15607; f) L. Cai, J. Yang, Y. Lai, Y. Liang, R. Zhang, C. Gu, S. Kitagawa, P. Yin, *Angew. Chem. Int. Ed.* **2023**, *62*, e202211747; *Angew. Chem.* **2023**, *135*, e202211747.

[7] a) Z. H. Li, H. Zeng, G. Zeng, C. Ru, G. Li, W. Yan, Z. Shi, S. Feng, *Angew. Chem. Int. Ed.* **2021**, *60*, 26577-26581; *Angew. Chem.* **2021**, *133*, 26781-26785; b) L. Liu, L. Yin, D. Cheng, S. Zhao, H. Y. Zang, N. Zhang, G. Zhu, *Angew. Chem. Int. Ed.* **2021**, *60*, 14875-14880; *Angew. Chem.* **2021**, *133*, 15001-15006; c) S. Chai, F. Xu, R. Zhang, X. Wang, L. Zhai, X. Li, H. Qian, L. Wu, H. Li, *J. Am. Chem. Soc.* **2021**, *143*, 21433-21442; d) S. Tao, L. Zhai, A. D. Dinga Wonanke, M. A. Addicoat, Q. Jiang, D. Jiang, *Nat. Commun.* **2020**, *11*, 1981; e) J. Zhang, Y. Kong, Y. Liu, H. Luo, Y. Zou, S. Zang, X. Ren, *ACS Materials. Lett.* **2022**, *4*, 2597-2603; f) K. A. Mauritz, R. B. Moore, *Chem. Rev.* **2004**, *104*, 4535-4585; g) F. Yang, G. Xu, Y. Dou, B. Wang, H. Zhang, H. Wu, W. Zhou, J. Li, B. Chen, *Nat. Energy.* **2017**, *2*, 877-883. g) F. Yang, G. Xu, Y. Dou, B. Wang, H. Zhang, H. Wu, W. Zhou, J. Li, Lin, R. Chen, G. Zhang, T. Huang, J. Li, X. Yang, L. Chung, L. Yu; J. He, *Appl. Mater. Interfaces* **2022**, *14*, 31942-31950.

[8] B. Shi, X. Pang, S. Li, H. Wu, J. Shen, X. Wang, C. Fan, L. Cao, T. Zhu, M. Qiu, Z. Yin, Y. Kong, Y. Liu, M. Zhang, Y. Liu, F. Pan, Z. Jiang, *Nat. Commun.* **2022**, *13*, 6666.

[9] a) D.-W. Lim, H. Kitagawa, *Chem. Rev.* **2020**, *120*, 8416-8467; b) P. G. M. Mileo, K. Adil, L. Davis, A. Cadiau, Y. Belmabkhout, H. Aggarwal, G. Maurin, M. Eddaoudi, S. Devautour-Vinot, *J. Am. Chem. Soc.* **2018**, *140*, 13156-13160.

[10] R. Sahoo, S. C. Pal, M. C. Das, *ACS Energy. Lett.* **2022**, *7*, 4490−4500.

[11] a) D. Gui, X. Dai, Z. Tao, T. Zheng, X. Wang, M. A. Silver, J. Shu, L. Chen, Y. Wang, T. Zhang, J. Xie, L. Zou, Y. Xia, J. Zhang, J. Zhang, L. Zhao, J. Diwu, R. Zhou, Z. Chai, S. Wang, *J. Am. Chem. Soc.* **2018**, *140*, 6146-6155; b) X. Li, L. Dong, J. Liu, W. Ji, S. Li, Y. Lan, *Chem* **2020**, *6*, 2272-2282. c) J. Hu, H. Zhang, Z. Feng, Q. Luo, C. Wu, Y. Zhong, J. Li, L. Chung, W. Liao, J. He, *Chin. Chem. Lett.* **2022**, *33*, 3227-3230.

[12] a) H. Chen, H. Tu, C. Hu, Y. Liu, D. Dong, Y. Sun, Y. Dai, S. Wang, H. Qian, Z. Lin, L. Chen, *J. Am. Chem. Soc.* **2018**, *140*, 896−899; b) S. Zheng, C. Wu, L. Chung, H. Zhou, J. Hu, Z. Liu, Y. Wu, L. Yu, J. He, *ACS Energy. Lett*. **2023**, *8*, 3095-3101; c) Z. Guo, Y. Zhang, Y. Dong, J. Li, S. Li, P. Shao, X. Feng, B. Wang, *J. Am. Chem. Soc.* **2019**, *141*, 1923-1927. d) S. Zheng, C. Wu, L. Chung, H. Zhou, J. Hu, Z. Liu, Y. Wu, L. Yu, J. He, *ACS Energy Lett.* **2023**, *8*, 3095-3101.

[13] F. J. Uribe-Romo, C. J. Doonan, H. Furukawa, K. Oisaki, O. M. Yaghi, *J. Am. Chem. Soc.* **2011**, *133*, 11478-11481.

[14] a) Y. Yang, P. Zhang, L. Hao, P. Cheng, Y. Chen, Z. Zhang, *Angew. Chem. Int. Ed.* **2021**, *60*, 21838-21845; *Angew. Chem.* **2021**, *13,* 22009-22016; b) L. Liu, L. Yin, D. Cheng, S. Zhao, H. Y. Zang, N. Zhang, G. Zhu, *Angew. Chem. Int. Ed.* **2021**, *60*, 14875-14880; *Angew. Chem.* **2021**, *133*, 15001-15006; c) S. Yang, C. Yang, C. Dun, H. Mao, R. S. H. Khoo, L. M. Klivansky, J. A. Reimer, J. J. Urban, J. Zhang, Y. Liu, *J. Am. Chem. Soc.* **2022**, *144*, 9827-9835; d) C. Fan, H. Wu, J. Guan, X. You, C. Yang, X. Wang, L. Cao, B. Shi, Q. Peng, Y. Kong, Y. Wu, N. A. Khan, Z. Jiang, *Angew. Chem. Int. Ed.* **2021**, *60*, 18051-18058; *Angew. Chem.* **2021**, *133*, 18199-18206; e) Z. Wang, Y. Yang, Z. Zhao, P. Zhang, Y. Zhang, J. Liu, S. Ma, P. Cheng, Y. Chen, Z. Zhang, *Nat. Commun.* **2021**, *12*, 1982; f) W. Zou, G. Jiang, W. Zhang, L. Zhang, Z. Cui, H. Song, Z. Liang, L. Du, *Adv. Funct. Mater.* **2023**,

10.1002/anie.202421444

33, 2213642; g) Z. Lu, C. Yang, L. He, J. Hong, C. Huang, T. Wu, X. Wang, Z. Wu, X. Liu, Z. Miao, B. Zeng, Y. Xu, C. Yuan, L. Dai, *J. Am. Chem. Soc.* **2022**, *144,* 9624-9633.
[15] a) X. Ge, Y. He, X. Liang, L. Wu, Y. Zhu, Z. Yang, M. Hu, T. Xu, *Nat. Commun.* **2018**, *9*, 2297; b) X. Liu, Y. Li, J. Xue, W. Zhu, J. Zhang, Y. Yin, Y. Qin, K. Jiao, Q. Du, B. Cheng, X. Zhuang, J. Li, M. D. Guiver, *Nat. Commun.* **2019**, *10*, 842; c) C. Ru, Z. Li, C. Zhao, Y. Duan, Z. Zhuang, F. Bu, H. Na, *ACS Appl. Mater. Interfaces.* **2018**, *10*, 7963-7973; d) S. Gahlot, V. Kulshrestha, *ACS Appl. Mater. Interfaces.* **2014**, *7*, 264-272; e) F. Ublekov, H. Penchev, V. Georgiev, I. Radev, V. Sinigersky, *Mater. Lett.* **2014**, *135*, 5-7.
[16] J. Chen, Q. Mei, Y. Chen, C. Marsh, B. An, X. Han, I. P. Silverwood, M. Li, Y. C, M. He, X. Chen, W. Li, M. K-. Jones, D. Crawshaw, M. D. Frogley, S. J. Day, V. G-. Sakai, P. Manuel, A. J. R-Cuesta, S. Yang, M. Schröder, *J. Am. Chem. Soc.* **2022**, *144*, 11969−11974.
[17] L. Cao, H. Wu, Y. Cao, C. Fan, R. Zhao, X. He, P. Yang, B. Shi, X. You, Z. Jiang, *Adv. Mater*. **2020**, *32,* 2005565.
[18] A. V. Chernyak, S. G. Vasiliev, I. A. Avilova, V. I. Volkov, *Appl. Magn. Reson.* **2019**, *50*, 677-693.
[19] P. Honegger, M. E. D. Pietro, F. Castiglione, C. Vaccarini, A. Quant, O. Steinhauser, C. Schröder, A. Mele, *J. Phys. Chem. Lett.* **2021**, *12*, 8658-8663.
[20] R. Bell, J. Saunders, *Can. J. Chem.* **1970**, *48*, 1114-1122.
[21] T. Famprikis, P. Canepa, J. A. Dawson, M. S. Islam, C. Masquelier, *Nat. Mater.* **2019**, *18*, 1278-1291.

Topic Graphic Content

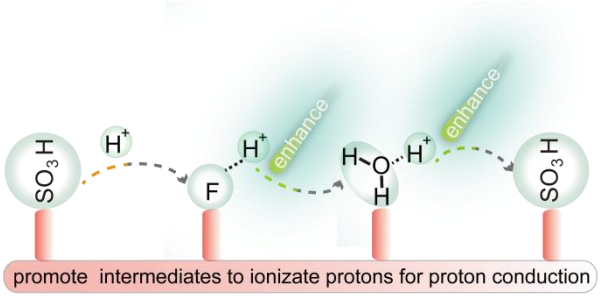

Although numerous studies on COF-based proton-conducting membranes have been documented, the majority concentrate on synthesis, with mechanistic investigations remaining relatively sparse. In addition, the mechanistic studies can be categorized into two primary areas. The first area is dedicated to the study of proton diffusion, including the analysis of hydrogen bonding patterns and the mobility of guest molecules. The second area delves into strategies to enhance the proton-dissociation capability of acidic groups, such as discussing the impact of electron-withdrawing groups or zwitterionic species. In this work, we meticulously study the role of proton intermediates in proton conduction and have successfully achieved superprotonic conductivity by reducing the proton dissociation energy of these intermediates.